

## Single-particle tunneling in semiconductor quantum dots

Y. M. Niquet,<sup>1,\*</sup> C. Delerue,<sup>1</sup> M. Lannoo,<sup>2</sup> and G. Allan<sup>1</sup>

<sup>1</sup>*Institut d'Electronique et de Microélectronique du Nord, Département ISEN, Boîte Postale 69, F-59652 Villeneuve d'Ascq Cedex, France*

<sup>2</sup>*Laboratoire Matériaux et Microélectronique de Provence, ISEM, Place G. Pompidou, 83000 Toulon, France*

(Received 14 June 2001; published 28 August 2001)

We present a calculation of single-charge tunneling in a semiconductor quantum dot based on a full self-consistent tight-binding calculation of the charging energies, applicable to quantum dots of realistic size (up to 8 nm diameter). Comparison with recent tunneling spectroscopy experiments on InAs nanocrystals shows excellent agreement and allows an unambiguous assignment of the conductance peaks. For bias voltages  $V$  larger than the band gap of the quantum dot we show that both electrons and holes can tunnel into the quantum dot, leading to specific features in the  $I(V)$  curves.

DOI: 10.1103/PhysRevB.64.113305

PACS number(s): 73.23.Hk, 73.63.Kv

Semiconductor nanocrystal quantum dots (QD's) represent the ultimate building blocks of optoelectronic and nanoelectronic devices. The reduction in size leads to quantum confinement, which results in a discrete, atomlike level structure and a blueshift of the optical band gap. It also enhances Coulomb charging effects that are significant in nano-sized transistors and memories. It is thus of major importance to realize such nanostructures in a well-controlled way, then study and try to understand their electronic properties. A major step in this direction has been achieved recently by Banin *et al.*,<sup>1</sup> who reported tunneling spectroscopy experiments on InAs nanocrystals that reveal rich features due to the interplay between quantum confinement and single-charge effects. Their interpretation allowed a convincing indexation of the electron tunneling peaks at positive bias voltages. However, it could not account for the multiplicity and splitting of these peaks at negative bias voltages. In this context the aim of the present Brief Report is to show that it is now possible to perform complete electronic structure calculations that allow a detailed understanding of the experimental data. The calculated QD band-gap energy and conduction band levels splittings agree extremely well with experiment over the whole range of sizes (2–8 nm). Our results point to the importance of taking into account tunneling of both electrons and holes at large bias voltages to get a full quantitative description of the observed spectrum. The discussion here will deal with the case of the InAs QD's of Ref. 1 but the method can be extended readily to other semiconductors.

We first recall some elements of the basic formalism describing tunneling spectroscopy in terms of the electronic structure of the QD. We use an extension of the theory of Averin *et al.*<sup>2</sup> that incorporates tunneling of both electrons and holes as well as electron-hole recombination. We then present our tight-binding (TB) electronic structure calculations and self-consistent treatment of the charging energies. Finally we refine the interpretation of the experimental  $I(V)$  curves and show that both electrons and holes tunnel into the QD at large bias voltages.

*Theory.* We consider a standard double barrier tunnel junction.<sup>3</sup> It consists of two metallic electrodes E1 and E2 weakly coupled to a semiconductor QD by two tunnel junctions J1 and J2 with capacitances  $C_1$  and  $C_2$ . The metallic electrodes E1 and E2 are characterized by their Fermi ener-

gies  $\varepsilon_F^1 = \varepsilon_F - eV$  and  $\varepsilon_F^2 = \varepsilon_F$ , where  $V$  is the bias voltage. The total energy of the QD charged with  $n$  electrons and  $p$  holes with respect to the neutral state can be written in the orthodox model<sup>3,4</sup> as

$$E(\{n_i\}, \{p_i\}, V) = \sum_i n_i \varepsilon_i^e - \sum_i p_i \varepsilon_i^h - \eta e V q + \frac{1}{2} U q^2. \quad (1)$$

$\varepsilon_i^e$  and  $\varepsilon_i^h$  are the conduction band (CB) and valence band (VB) energy levels of the QD,  $n_i$  and  $p_i$  are electron and hole occupation numbers ( $n = \sum_i n_i$ ,  $p = \sum_i p_i$ ),<sup>5</sup> and  $q = n - p$ . In terms of the junction capacitances  $C_1$  and  $C_2$ ,  $U = e^2 / (C_1 + C_2)$  is the charging energy, and  $\eta = C_1 / (C_1 + C_2)$  is the part of the bias voltage  $V$  that drops across junction J2 in the neutral QD. Tunneling of an electron onto the energy level  $\varepsilon_i^e$  occurs at transition energy

$$\begin{aligned} \varepsilon_i^e(q, q+1) &= E(n_i=1, \{p_j\}, V) - E(n_i=0, \{p_j\}, V) \\ &= \varepsilon_i^e - \eta e V + U(q + \frac{1}{2}), \end{aligned} \quad (2)$$

while tunneling out occurs at  $\varepsilon_i^e(q-1, q)$ . In the same way, hole tunneling in [out] occurs at  $\varepsilon_i^h(q-1, q)$  [ $\varepsilon_i^h(q, q+1)$ ]. The total tunneling rates through junction  $J\alpha$  ( $\alpha=1,2$ ) can be expressed<sup>6</sup> in terms of the tunneling rates  $\Gamma^\alpha$  onto levels  $\varepsilon_i^e$  and  $\varepsilon_i^h$  following the lines of Ref. 2. The difference with Ref. 2 is that we treat both electrons and holes at the same time and incorporate the electron-hole recombination rate  $R(n, p)$  from the charge state  $(n, p)$  to the charge state  $(n-1, p-1)$  into the master equations. At  $T \rightarrow 0$  K, the  $I(V)$  curve looks like a staircase.<sup>2,4</sup> It exhibits a step each time  $\varepsilon_F^1$  or  $\varepsilon_F^2$  crosses a transition energy  $\varepsilon_i^e(q, q+1)$  or  $\varepsilon_i^h(q-1, q)$ . Then a new charge state becomes available in the QD (addition step), or a new channel  $\varepsilon_i^e$  or  $\varepsilon_i^h$  is opened for tunneling to a given, already available charge state (excitation step).

This behavior is apparent in the results of Banin *et al.*,<sup>1</sup> who reported tunneling spectroscopy experiments on InAs nanocrystals. The differential conductance  $G(V) = dI(V)/dV$  is shown in Fig. 1 for a 6.4 nm diameter nanocrystal. The tip was retracted from the QD so that  $C_1/C_2$  is maximum and  $\eta$  is close to 1. A zero-current gap is observed around  $V=0$  followed by a series of conductance peaks for

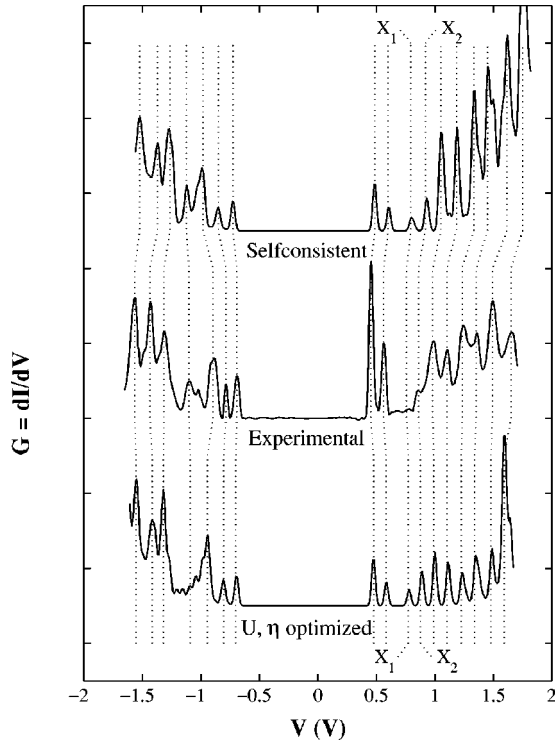


FIG. 1. Comparison between calculated and experimental differential conductance  $G(V)$  curves for a 6.4 nm diameter InAs nanocrystal. The optimized parameters for the capacitive model are  $U = 100$  meV and  $\eta = 0.9$  (see text).

$V < 0$  and  $V > 0$ . We now discuss the interpretation of this  $G(V)$  curve on the basis of our results and compare with Ref. 1.

**Electronic structure of InAs nanocrystals.** The energy levels  $\varepsilon_i^e$  and  $\varepsilon_i^h$  of spherical InAs nanocrystals are calculated with an orthogonal  $sp^3$  TB model with second-nearest neighbor interactions. The TB parameters are fitted to the bulk InAs band structure calculated with the local density approximation corrected from the band-gap problem, and to the experimental effective masses.<sup>7</sup> Spin-orbit coupling is included. The surface dangling bonds are saturated with pseudohydrogen atoms. As a first test of the accuracy of this description, we compare the calculated QD band-gap energy  $E_g^0$  with the tunneling spectroscopy data of Ref. 1. According to Eq. (3), the zero-current gap in the  $I(V)$  curve is  $\Delta V = (E_g^0 + U)/e\eta$ . Assuming  $\eta = 1$  (as in Ref. 1) and an independent determination of  $U$  (see below) gives an upper limit for  $E_g^0$  plotted in Fig. 2(a). The agreement with TB results is extremely good over the whole 2–8 nm diameter range, although the TB band-gap energy may be slightly overestimated. We find that the lowest CB level ( $1S_e$ ) is  $s$ -like, twofold degenerate, and the next CB level ( $1P_e$ ) is  $p$ -like, sixfold degenerate.<sup>8</sup> The highest two VB levels  $1V_B$  and  $2V_B$  are found fourfold degenerate. On this basis, for  $V > 0$ , Banin *et al.*<sup>1</sup> assigned the first group of two peaks (see Fig. 1) and second group of six peaks to the tunneling of electrons filling the  $1S_e$  and  $1P_e$  CB levels, respectively. The successive peaks in each group are thus found separated by the charging energy  $U/e\eta$ , and the two groups by  $(\Delta_{CB} + U)/e\eta$ , where

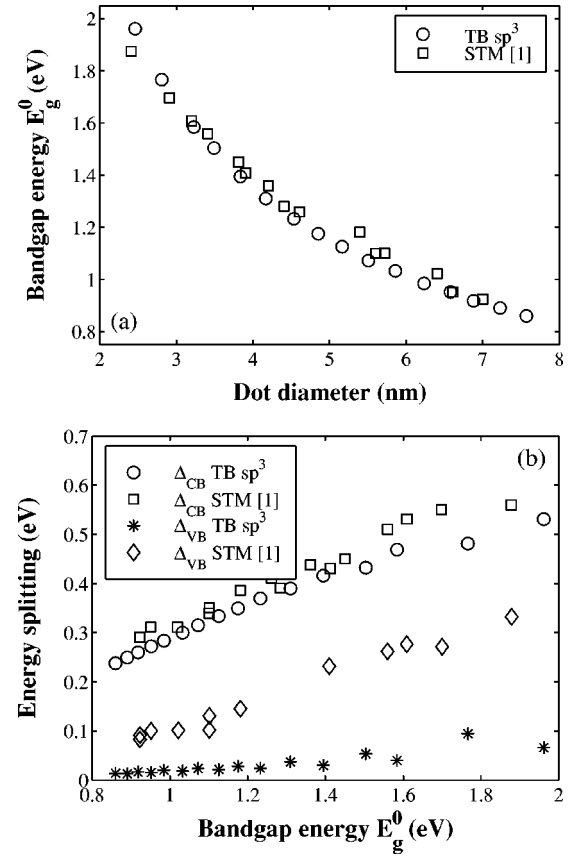


FIG. 2. (a) Comparison between the calculated (TB) and experimental [STM (Ref. 1)] band-gap energy  $E_g^0$  versus size. (b) Comparison between the calculated and experimental energy splittings  $\Delta_{CB}$  and  $\Delta_{VB}$  versus  $E_g^0$  (see text).

$\Delta_{CB} = \varepsilon(1P_e) - \varepsilon(1S_e)$ . For  $V < 0$ , they assigned the first group of four peaks and next group of three intense peaks to the tunneling of holes filling the  $1V_B$  and  $2V_B$  VB levels, respectively. These groups are thus found separated by  $(\Delta_{VB} + U)/e\eta$ , where  $\Delta_{VB} = \varepsilon(2V_B) - \varepsilon(1V_B)$ . An upper limit ( $\eta = 1$ ) for the splittings  $\Delta_{CB}$  and  $\Delta_{VB}$  is plotted in Fig. 2(b) versus the band-gap energy  $E_g^0$  and compared to our predictions. For  $\Delta_{CB}$  the agreement is striking so that our results support the previous interpretation for  $V > 0$ . On the other hand, the calculated  $\Delta_{VB}$  is much lower than the experimental one. This discrepancy added to the fact that the multiplicity of the first group of peaks for  $V < 0$  is not the same from dot to dot (and is sometimes found odd) leads us to question the simple interpretation of Ref. 1 in terms of pure single-hole tunneling. A full calculation of the  $I(V)$  curves is thus needed for a complete understanding of the tunneling spectroscopy data.

**Calculation of the  $I(V)$  curves.** For the sake of comparison with the interpretation of Ref. 1 we perform two types of calculations: (i) we use the capacitive model of Eq. (1) with our calculated TB level structure and consider  $U$  and  $\eta$  as fitting parameters chosen to optimize the agreement with the position of the peaks in the  $G(V)$  curve. (ii) we make a fully self-consistent treatment on a system with a realistic geometry described below and shown in the inset of Fig. 3. Here

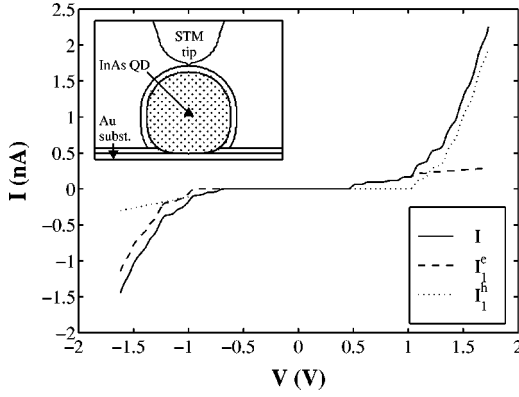


FIG. 3. Self-consistent  $I(V)$  curve for the geometry of the inset showing the electron ( $I_1^e$ ) and hole ( $I_1^h$ ) currents through junction J1.

the ground state energy  $E_0(n, p, V)$  is self-consistently calculated for a set of charge states  $(n, p)$  and bias voltages  $V_i$ . This is done in the Hartree approximation corrected from the unphysical self-interaction term.<sup>6</sup> Other exchange and correlation terms are not included, since they are much smaller<sup>9</sup> and are not seen in the present experiments. The electrostatic potential inside the QD is computed with a finite difference method. The calculation is performed in the subspace spanned by the highest  $N_{VB}$  VB states and lowest  $N_{CB}$  CB states of the isolated QD. The transition energies are derived from Eq. (2). The ground state energy is interpolated over the whole bias voltage range and excited configuration energies  $E(\{n_i\}, \{p_i\}, V)$  are approximated from the spectrum of the self-consistent ground state Hamiltonian and interpolated between successive  $V_i$ . The charging energies  $U$  calculated with this method are in good agreement with the experimental ones.<sup>1,6</sup>

For the capacitive model, we consider a spherical 6.4 nm diameter InAs nanocrystal. We get  $\varepsilon(1S_e) = 0.848$  eV,  $\varepsilon(1P_e) = 1.120$  eV,  $\varepsilon(1VB) = -0.105$  eV, and  $\varepsilon(2VB) = -0.120$  eV. For the self-consistent calculation we get better results with a slightly flattened dot as shown in the inset of Fig. 3. This does not significantly change the electronic structure of the QD but only the details of the electrostatic potential. The dielectric constant of the QD  $\varepsilon_r = 13.6$  is calculated as in Ref. 10. The QD is linked to the gold substrate (E1) by a 5 Å thick hexane dithiol layer and is surrounded by a 5 Å thick layer of molecular ligands ( $\varepsilon_r = 2.6$ ). The radius of curvature of the Pt-Ir scanning tunneling microscope (STM) tip (E2) is  $r = 2.5$  nm, and the tip-QD distance is  $d = 5$  Å. Taking  $N_{VB} = 240$  and  $N_{CB} = 120$  ensures convergence of the self-consistent calculation. The zero-bias Fermi energy  $\varepsilon_F = 0.5$  eV is obtained from the position of the center of the zero-current gap.<sup>11</sup> A detailed analysis of the relative height of the low-lying current steps around the zero-current gap suggests that  $\Gamma^1 \approx \Gamma^2$ . Since an accurate calculation of the tunneling rates  $\Gamma^\alpha$  is not possible, we set  $\Gamma^1 = \Gamma^2 = 6 \times 10^8$  s<sup>-1</sup> for electrons and  $\Gamma^1 = \Gamma^2 = 3 \times 10^8$  s<sup>-1</sup> for holes to get a correct order of magnitude of the current. It is important to note that the position of the calculated conductance peaks does not depend on the tunnel-

ing rates  $\Gamma^\alpha$ . Last, we set  $R(n, p) = np/\tau$  and  $\tau = 1$  ns, which is characteristic of direct gap semiconductors.

**Results and discussion.** The calculated  $G(V)$  curves are compared to the experimental one in Fig. 1. They are broadened with a Gaussian of width  $\sigma = 15$  meV. The optimized parameters for the capacitive model are  $U = 100$  meV and  $\eta = 0.9$  ( $C_1 = 1.44$  aF,  $C_2 = 0.16$  aF). As shown in Fig. 1 the agreement with experiment is extremely good with practically a one to one correspondance between the calculated and experimental peaks over a range of 3.5 V. The negative bias voltages side is clearly improved in the self-consistent calculation. However, in that case there is a slight shift of the peaks but the results are quite sensitive to the details of the geometry, which is not known precisely, so we have not tried to improve the agreement with experiment further. We can use Eqs. (1)–(3) to analyze the nature of the current. For small  $|V|$  just beyond the zero-current gap, electrons (holes) first tunnel from the STM tip into the QD when  $V > 0$  ( $V < 0$ ). In these conditions, either conduction or valence band energy levels are readily inferred from the  $G(V)$  curve. When increasing further  $|V|$ , a new regime appears where both electrons and holes tunnel into the QD, making the interpretation of the  $I(V)$  curve more intricate. This is evidenced by the following arguments, given for  $V > 0$ . An electron can tunnel from the STM tip (E2) into the QD charged with  $n - 1$  electrons as soon as

$$\varepsilon_F^2 \geq \varepsilon_n^e(n - 1, n) = \varepsilon_n^e - \eta eV + (n - \frac{1}{2})U. \quad (4)$$

Then a first hole can tunnel from the gold substrate (E1) into the QD now charged with  $n$  electrons if

$$\varepsilon_F^1 \leq \varepsilon_1^h(n - 1, n) = \varepsilon_1^h - \eta eV + (n - \frac{1}{2})U. \quad (5)$$

Subtracting Eqs. (4) and (5) one finds that the tunneling of holes in the QD charged with  $n$  electrons is possible only if

$$eV = \varepsilon_F^2 - \varepsilon_F^1 \geq \varepsilon_n^e - \varepsilon_1^h \geq E_g^0. \quad (6)$$

Similar relations can be derived for  $V < 0$ , electrons tunneling from the gold substrate into the QD at large bias voltages. Therefore, in any tunneling spectroscopy experiment with charging, the tunneling of either electrons or holes alone is ensured only if  $e|V|$  is below the band-gap energy  $E_g^0$  of the QD. Tunneling of both electrons and holes below  $-0.94$  V and above 1.08 V is seen<sup>12</sup> in Fig. 3.

We can now proceed to a more detailed analysis of the  $G(V)$  curves. For  $V > 0$ , the first group of two peaks is assigned to the tunneling of electrons filling the  $1S_e$  CB level, and the next group of six peaks to the tunneling of electrons through the  $1P_e$  CB level and tunneling of holes. There are also two excitation peaks  $X_1$  and  $X_2$  on Fig. 1 (tunneling through the  $1P_e$  CB level in the charge states  $n = 0$  and  $n = 1$ ) that are hardly visible on the experimental  $G(V)$  curve but disappear at higher  $\Gamma^2/\Gamma^1$  ratios. As can be seen in Fig. 1, we overestimate the amplitude of the current at large positive bias voltages. Better agreement could be achieved in this range simply dividing  $\Gamma^1$  by 4 for holes. This may arise because the self-consistent calculation shows that the hole states strongly localize near the STM tip at positive bias. For

$V < 0$ , the first two peaks can be unambiguously assigned to the tunneling of holes filling the  $1_{VB}$  VB level. However, the next group of peaks is a very intricate structure involving single-hole charging peaks and tunneling of electrons through the  $1S_e$  CB level. This disagrees with the interpretation of Ref. 1 in terms of single-hole tunneling and makes any experimental determination of  $\Delta_{VB}$  ill-defined. This also means that the multiplicity of the peaks is not reproducible as found experimentally. Finally, the strong increase of the current below  $-1.25$  V is mainly related to the tunneling of electrons through the  $1P_e$  CB level.

In conclusion, we have performed self-consistent tight-binding calculations for InAs QD's. The calculated QD

band-gap energy, conduction band levels splittings, and charging energies are in excellent agreement with experiment over the whole range of sizes (2–8 nm), and the calculated tunneling spectra allow a detailed assignation of the conductance peaks. Let us recall that the possible tunneling of both electrons and holes should be kept in mind in any tunneling spectroscopy experiment performed at bias voltages larger than the band-gap energy of the QD.

The Institut d'Electronique et de Microélectronique du Nord is UMR 8520 of CNRS and the Laboratoire Matériaux et Microélectronique de Provence is UMR 6137 of CNRS. We thank O. Millo for fruitful discussions.

---

\*Electronic address: niquet@isen.iemn.univ-lille1.fr

<sup>1</sup>U. Banin, Y. Cao, D. Katz, and O. Millo, *Nature* (London) **400**, 542 (1999).

<sup>2</sup>D.V. Averin, A.N. Korotkov, and K.K. Likharev, *Phys. Rev. B* **44**, 6199 (1991).

<sup>3</sup>*Single-Charge Tunneling: Coulomb Blockade Phenomena in Nanostructures*, edited by H. Grabert and M. Devoret (Plenum, New York, 1992).

<sup>4</sup>R.I. Shekhter, *Zh. Éksp. Teor Fiz.* **63**, 1410 (1972) [*Sov. Phys. JETP* **36**, 747 (1973)]; I.O. Kulik and R.I. Shekhter, *ibid.* **68**, 623 (1975) [*ibid.* **41**, 308 (1975)].

<sup>5</sup>Spin and other degeneracies are included in the single index  $i$ ; therefore  $n_i, p_i \in \{0, 1\}$ .

<sup>6</sup>Y.M. Niquet, C. Delerue, G. Allan, and M. Lannoo (unpublished).

<sup>7</sup>Y.M. Niquet, C. Delerue, G. Allan, and M. Lannoo, *Phys. Rev. B*

**62**, 5109 (2000).

<sup>8</sup>In fact, spin-orbit coupling splits this sixfold degenerate  $p$ -like state into one twofold and one fourfold degenerate state.

<sup>9</sup>A. Franceschetti, A. Williamson, and A. Zunger, *J. Phys. Chem.* **104**, 3398 (2000).

<sup>10</sup>M. Lannoo, C. Delerue, and G. Allan, *Phys. Rev. Lett.* **74**, 3415 (1995).

<sup>11</sup>We have taken into account a 0.5 V built-in potential in the self-consistent calculation (work-function difference between electrodes E1 and E2). However, this built-in potential has minor influence on the  $I(V)$  curves.

<sup>12</sup>In fact, the band-gap energy of the QD is slightly lowered by the tip-induced electric field, which explains why tunneling of both electrons and holes occurs a bit earlier than expected from Eq. (6) in the self-consistent calculation.